第 26 卷第 3 期 无 机 化 学 学 报 Vol.26 No.3
2010 年 3 月 CHINESE JOURNAL OF INORGANIC CHEMISTRY 365-373

纳米框诱导的三角形纳米银片合成

王悦辉*,[1,2] 张 琦[1] 王 婷[1,3] 周 济*,[1]
([1]清华大学新型陶瓷与精细工艺国家重点实验室,北京 100084)
([2]电子科技大学中山学院化学与生物系,中山 528402)
([3]北京有色金属研究总院,北京 100088)

摘要:以二异辛基磺化琥珀酸钠(CAS No.577-11-7,1,4-二(2-乙基己基)丁二酸酯磺酸钠盐 Bis(2-ethylhexyl) sulfosuccinate sodium salt, Dioctyl sulfosuccinate sodium salt,AOT)和柠檬酸钠为表面修饰剂,在 60 ℃及 36~50 h 的水浴条件下采用硼氢化钠还原硝酸银合成出高产率形貌规则的三角形纳米银片。通过控制反应条件可以在边长 600~400 nm,厚度 5~20 nm 范围内调控三角形纳米银片尺寸。通过三角形纳米银片合成过程的显微结构表征提出了三角形框诱导的三角形纳米银片融合生长机制。在 AOT 表面修饰剂作用下,纳米银粒子自组装融合生长形成三角形纳米框。小的纳米银粒子的融合、消耗促进三角形纳米框形成三角形纳米片。AOT 浓度、反应时间和溶液 pH 值等因素的研究进一步表明了在一定的条件下以三角形框形成为基础的三角形纳米银片的融合生长机制。

关键词:三角形纳米银片;纳米框;AOT;诱导合成
中图分类号:O614.122;O647.3 **文献标识码**:A **文章编号**:1001-4861(2010)03-0365-09

Nanoframes Directed Synthesis of Triangular Silver Nanoplates

WANG Yue-Hui*,[1,2] ZHANG Qi[1] WANG Ting[1,3] ZHOU Ji*,[1]
([1]*State Key Laboratory of New Ceramics and Fine Processing, Department of Materials Science and Engineering, Tsinghua University, Beijing* 100084)
([2]*Department of Chemistry and Biology, University of Electronic Science and Technology of China Zhongshan Institute, Zhongshan, Guangdong* 528402)
([3]*Beijing General Research Institute for Nonferrous Metals, Beijing* 100088)

Abstract: A simple and effective aqueous-phase approach was used for a large-scale synthesis of regular silver triangular nanoplate, which is with a thickness of 5~20 nm and a size tunable from 60 to 400 nm. The standard synthesis process involved the reduction of silver nitrate with sodium borohydride in the presence of sodium citrate and dioctyl sulfosuccinate sodium salt(AOT, CAS No.577-11-7; Bis(2-ethylhexyl) sulfosuccinate sodium salt,) and heat-treatment at 60 ℃ for 36~50 h. The studies of the growth process indicate that the silver triangular nanoframes form in the formation process, serving as templates for triangular nanoplates. The formation process of triangular nanoframes is involved with nanoparticles assembly due to the interaction with AOT. In addition, the heating provides a driving force to facilitate the Ostwald ripening process-growth of these triangular nanoframes at the expense of some nanoparticles and incorporation of nanoparticles. Studies from different AOT concentrations, pH values and reaction time demonstrate that triangular nanoframe-mediated growth mechanism works only in the proper experimental conditions.

Key words: silver nanoplates; nanoframes; AOT; directed synthesis

收稿日期:2009-10-19。收修改稿日期:2009-12-26。
国家自然科学基金(No.50272032)和广东省自然科学基金(No.7300212)项目和电子科技大学中山学院科研启动基金项目资助。
*通讯联系人。E-mail:zhouji@mail.tsinghua.edu.cn; wangzsedu@126.com
第一作者:王悦辉,女,35 岁,副教授;研究方向:信息功能材料及光电材料。

In recent years, much research and development has been focused on the growth and properties of two-dimensional silver (Ag) nanomaterials due to their amazing ability to control optical properties and their promising applications in optics, photonics, and biotechnology[1-5]. Much effort has been devoted to the synthesis of Ag nanoplates and nanoprisms[6-14]. The room temperature transformation of spherical nanoparicles into nanoprisms and triangular nanoplates can be performed out using UV light and irradiation[15-17] or by a thermal process[7,12-13,18-19]. Callengari et al.[20] described a photochemical conversion process in which spherical Ag nanoparticles were converted into triangular plates of various sizes after irradiation with a light of appropriate wavelength. Other methods for preparation of Ag nanoplates include seed-mediated growth in the presence of cetyltrimethylammonium bromide (CTAB) soft templates[21] and by boiling a dimethyl formamide (DMF) solution of $AgNO_3$ in the presence of poly(*N*-vinyl-2-pyrrolidone)(PVP).[13] While the synthesis of Ag triangular nanoplate has been successful in many cases, well-defined, systematic control of the size of nanoplates, (i.e., the control of crystal growth in two dimensions) has shown to be much more difficult. This is due to the reason that the Ag triangular nanoplate is a thermodynamically unfavorable shape.

With the diversity of synthesis methods have come to a number of mechanistic explanations for the formation of the thermodynamically unfavorable shape. The proposed mechanisms seem to fall into three general categories. One explanation suggests that high concentrations of surfactant create micelles, which acts as templates for crystal growth and as space-confining structures that lend their shape to the growing colloid[10,22-25]. The second explanation involves the growth regulation kinetically of specific crystal faces by chemically adsorbed molecules due to hindering or accelerating the addition of atoms to specific crystal planes[4-9,26-27]. The third mechanism explains that the presence and orientation of twin planes in the face-centered cubic (FCC) metals direct the shape of the growing particles[28].

In this paper, we report a new simple and effective aqueous-phase approach for the large-scale synthesis of regular silver triangular nanoplates with the size tunable from 60 to 400 nm. The optical in-plane dipole plasmon band of the large nanoplate (with a mean diameter more than 150 nm) has been extended to ca. 1230 nm, which is in the near-infrared (NIR) regime. This extension has made the large nanoplates ideal for photothermally triggered drug releasing in tissues and in IR absorption or optical fiber communication. Meanwhile, it is interesting to find the triangular nanoplates formed through triangular nanoframes as intermediate product, which serves as the template in directing the formation of triangular nanoplates. To the best of our knowledge, this shape evolution has not been reported and and is deserving of further investigation as a process of anisotropic nanoparticles.

1 Experimental

1.1 Materials

Silver nitrate ($AgNO_3$, 99.8%), sodium citrate ($Na_3C_6H_5O_7$, 99%), and sodium borohydride ($NaBH_4$, 98%) were purchased from Beijing Chemical Reagent Co., Ltd. (China). Dioctyl sulfosuccinate sodium salt (AOT, 99.5% , CAS No. 577-11-7, Bis (2-ethylhexyl) sulfosuccinate sodium salt) was purchased from Alfa Aesar China (Tianjin) Co., Ltd. All the reagents used were of analytical purity and were used as received.

1.2 Synthesis of silver triangular nanoplates

In a standard condition, 50 mL of 1 mmol·L^{-1} $AgNO_3$ and 2 mmol·L^{-1} $Na_3C_6H_5O_7$ were mixed with 50 mL 1 mg·L^{-1} aqueous solution of AOT. The mixture solution was stirred for 15 min to form a homogeneous mixture at ambient laboratory condition. 0.1 mL of ice-cold 0.01 mmol·L^{-1} $NaBH_4$ was then rapidly injected into the vigorously stirred solution with glass syringe and the solution turned yellow. The solution was further stirred for another 5 min. The pH value of the solution was about 7 at this time. The reaction solution was then heated at 60 ℃ in constant temperature water bath pot for 48 h(note that the solution was not stirred during the entire heating process). During the whole reaction process, the color of the colloidal solution changed from

light yellow to brown, red, purple, deep purple-red, green, and finally to blue. Ag nanoplates could be separated from the spherical nanoparticles by centrifuging. The product was consisted of triangular nanoplates(~90%) and spheres(~10%) by centrifuging at 4 800 r·min^{-1} for 30 min, but was consisted of more than 97% triangular nanoplates by centrifuging at 8 000 r·min^{-1} for 20 min. The nanoplates size was tuned by changing the reaction time. For the mechanism studies, some experimental parameters were changed while keeping other parameters constant.

1.3 Structural characterization

All TEM images were taken using a JEOL 200CX TEM operated at 200 kV. High-resolution transmission electron microscopy(HRTEM) images were taken on a JEOL 2011 HRTEM operated at 200 kV. For TEM measurements, the samples were prepared by dropping the solution on carbon-coated copper grids and let dry in air. XRD patterns of the nanoplates were recorded by using a Rigaku D8-Discover diffractometer equipped with Cu $K\alpha$ radiation(λ=0.154 18 nm) and a graphite monochromator at a scanning rate of 0.02° per second in 2θ ranging from 25° to 85°. XRD measurement was prepared by placing a colloidal solution on glass and let dry in air. The UV-visible-infrared absorption spectra were obtained using a UNICAM UV-500 PC (The United States) spectropho-tometer and Perkin Elmer Lambda950 UV-VIS-NIR (The United States) Spectrometer and a quartz cuvette with a 1-cm optical length.

2 Results and discussion

2.1 Microscopic and spectroscopic monitoring of the growth process

The Ag nanostructures at various stages of the formation process were traced by the UV-Vis spectra and TEM micrographs. Fig.1 shows TEM images of the samples taken from the reaction solution after the reaction solution is heated at 60 ℃ for different reaction times (Note that all samples are purified by centrifugation under the same conditions). In our experiments, AOT is used as a surfactant, which is

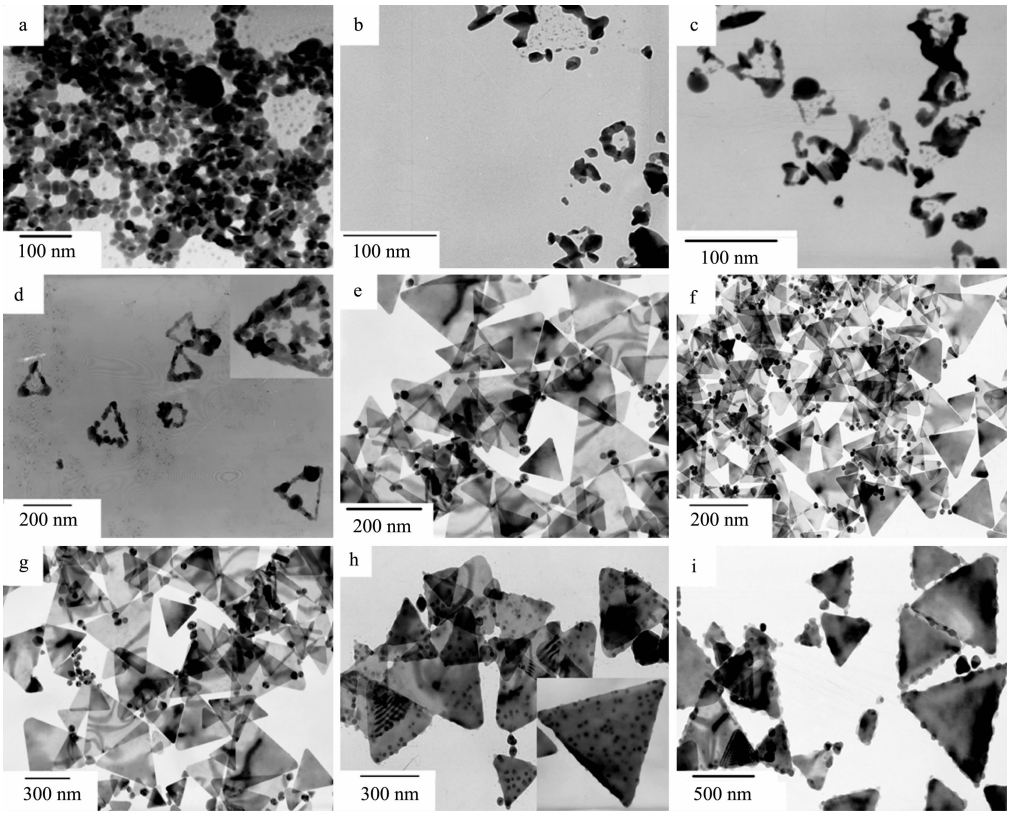

(a) 6; (b) 14; (c) 25; (d)30; (e)36; (f) 42; (g) 48; (h) 56; (i) 72 h

Fig.1　TEM images of silver nanostrucutures at different reaction times All solutions were purified by centrifugation

dynamically adsorbed and desorbed on the particle surface to control the morphology of particle in the course of crystal growth. It is clear that the nanostructures size and shape of nanostructures change remarkably in the whole reaction process. When the reaction has proceeded for 6 h, the reaction solution is slowly darkened to a brown solution by heating and the spherical Ag nanoparticles are formed with an average diameter of 30 nm as shown in Fig.1a. At 14 h, the spherical particles aggregates, with a small amount of unintegrated triangular nanoframes(Fig.1b), are formed. At 25 h, the reaction solution becomes green; more unintegrated triangular nanoframes are observed, companying with a progressive growth in nanoframes size and the decrease in nanoparticles (Fig.1c). This phenomenon agrees well with the known characteristics of Ostwald ripening of forming large particles by "dissolving" smaller particles. It is noted that triangular nanoframes are formed not only by aggregating of nanoparticles due to self-assembly but also by dissolving of small nanopartilces due to the Ostwald ripening process. It has been reported that Ag nanoparticles could assemble themselves into a largely linear fashion drived by surfactants[31]. After 30 h, the reaction solution becomes deep-green after centrifugation and separation, the product solution becomes blue, and many integrated triangular nanoframes with size of 150 ~200 nm are the main products. From Fig.1d, the nanoparticles grown on the edges of triangular nanoframes and some incorporated nanoparticles filled in the nanoframes(inset in Fig.1d) are observed. Some small particles with size below 10 nm are also observed surrounding nanoframes. It is supposed that these small particles may play an important role in the formation of triangular nanoframes through an "Ostwald ripening" process. After 36 h, many irregular triangular nanoplates with size of 150~250 nm are observed (Fig. 1e). After 40 h, many triangular nanoplates with perfectly sharp corners and shape regularity with edge length from 100~250 nm are observed. Meanwhile, nanospheres with an average diameter of 20 nm are present among a majority of triangular nanoplates(Fig.1f). After 48 h, the triangular nanoplates with regular shape are still main products, obviously larger than those at 40 h (Fig.1g). After 56 h, many triangular nanoplates adsorbed on small nanospheres with mean diameter of 10 nm are observed (Fig.1h). It is worth noting that the edges of triangular nanoplates are not smooth. It is supposed that some of the Ag atoms are dissolved as Ag^+, and it nucleates and grows again on the surfaces of the nanoplates. After 72 h, the similar products as 56 h are observed except that the size of triangular is larger than that of 56 h. The set of experiments demonstrates that a proper time is necessary for the formation of the regular triangular nanoplates, and the size and morphology of the nanoplates are able to be tuned by controlling the reaction time.

Fig.2 shows UV-Vis-Infrared spectra obtained under the same conditions as that speified in Fig.1. When the reaction time is extended for 6 h(Fig.2a curve

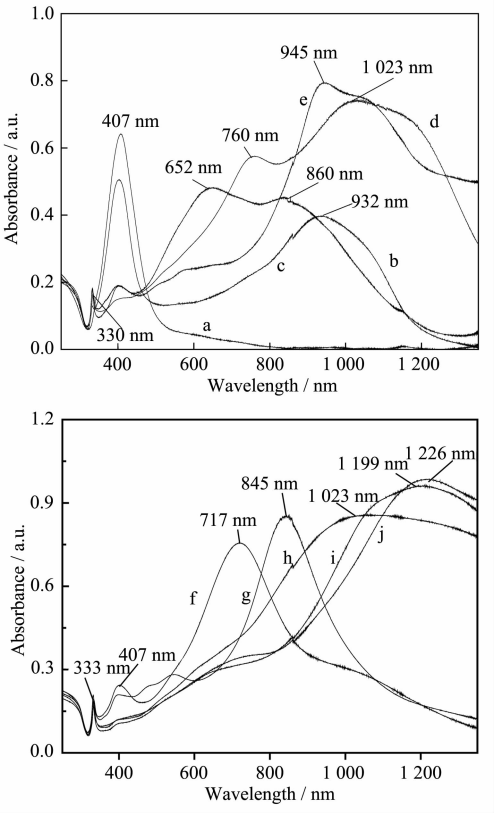

(a) 6; (b) 14; (c) 25; (d) 30; (e) 36; (f) 42; (g) 48; (h) 56; (i) 60; (j) 72 h

Fig.2 Absorption spectra of the reaction solution under standard condition at various reaction times: All solutions are purified by centrifugation and separation

a), there is a very remarkable symmetric absorption peak centered at 407 nm, showing that the solution contains small Ag nanoparticles with uniform size, which is proved by the TEM image shown in Fig.1a. After 14 h (Fig.2a curve b), the symmetric absorption peak of silver nanoparticles still presents with a much weaker absorption peak at 333 nm and a very stronger broad absorption peak centered at 932 nm because of the appearance of some anisotropic nanoparticles. Based on the TEM results, the peak at 333 nm can be attributed to the triangular nanoframes, while the broad band at 932 nm might not only arise from the triangular nanoframes but also could be attributed to the aggregation of nanoparticles [29]. When the reaction proceeds to 25 h, four peaks at 333 nm (weak), 407 nm (weak), 578 nm(strong), and 850 nm(strong) is observed in the UV-Vis-Infrared spectrum (Fig.2a curve c). It is important to note that the characterization of the UV-Vis-Infrared spectrum agrees with that of surface plasmon resonance (SPR) of the triangular nanoplate. Seen from TEM image, triangular nanoframes are the main products at this time, so we can come to a conclusion that the triangular nanoframe has similar SPR with the triangular nanoplate. Triangular nanoframe is formed by self-assembly of nanoparticles. Such a linear self-assembly of nanoparticles helps us to explain the origin of the SPR by means of a dipolar interaction mechanism. The perturbed charge distribution on assembled Ag nanoparticles in the presence of external electromagnetic radiation results in an additional attractive force between the polarized negative and positive charges on adjacent particles. This additional attractive interaction derives higher order of SPR[30].

When the reaction is extended to 30 h, two peaks at 652 and 845 nm are red-shifted to 760 and 1 023 nm, respectively(Fig.2a curve d). At the same time, the peak intensity ratio in range of 760 nm to 1 023 nm is higher than that reacted for 25 h. This is because the triangular nanoframe is larger and more regular at this time. When the reaction proceeds to 36 h, four peaks at 945 nm, 578 nm, 407 nm, and 333 nm are observed in UV-Vis-IR spectrum(Fig.2a curve e). According to TEM images, the main products are triangular nanoplates and nanosphere at this time. The peak at 407 nm could be attributed to the SPR of small spherical nanoparticles, and others could be attributed to the SPR of triangular nanoplates. Based on theoretical calculations by Schatz et al [31], the 333 nm peak is the out-plane quadrupole plasmon resonance, the 578 nm peak is the in-plane quadrupole plasmon resonance, and the 945 nm peak is the in-plane dipole plasmon resonance. The relative intensity of the 945 nm peak is much stronger than what expects theoretically. It implies the existence of aggregates in the solution. As the reaction proceeds to 42 h, the solution exhibits three distinct peaks located at 333, 407, and 717 nm, which is typical of the SPR for a perfect triangular silver nanoplate (Fig.2b curve f). When the reaction proceeds to 48 h, triangular silver nanoplates continue to grow. The in-plane dipole resonance band is greatly red-shifted from 717 nm to 845 nm(Fig.2b curve g). If the reaction is completed at 48 h, the final product is regular triangular nanoparticles with a size from 150 to 400 nm. In the period from 56 to 72 h, the broad peaks in the NIR region (Fig.2b, curve h, i, j) are observed in UV-Vis-Infrared spectra. These peaks arise from the in-plane dipole resonance mode associated with silver nanoplates whose edge length exceeds 100 nm and the aggregation of silver nanoplatets, which could induce a strong coupling between individual plates [7]. The peak further red-shifts from 1 023 to 1 226 nm with time. This result is consistent with theoretical predictions that the dipole resonance mode could be significantly red-shifted with the increase in nanoplate size. The intensity of the peak around 407 nm is quite weak. This is because that the spherical nanoparticles are absorbed on the surface of triangular nanoplate, and their SPR is hindden due to the much stronger SPR of triangular nanoplates. It is worth noting that the peak at 333 nm does not change during all the reaction process. This result indicates that the out-plane quadrupole plasmon resonance is not affected by the morphology and size of triangular nanoplate.

The photos of as-prepared silver triangular nanoplates with the different sizes (after centrifugation),

i.e. (i) 100 nm, (ii) 150 nm, (iii) 200 nm and (iv) 250 nm, are shown in Fig.3a. It is clear that the color of silver triangular nanoplates solution is blue, and the difference is observed with the change of size. Flat structures such as thin films grown on various substrates often exhibit Moiré patterns when their TEM images are recorded. Moiré patterns could also be observed when two or more nanoplates are stacked against their triangular faces with tight contact. Fig.3b shows typical example of Moiré pattern for an array of parallel lines. The formation of these patterns can be attributed to the difference in orientation between the two silver nanoplates. The electron diffraction pattern of an individual flat-lying nanoplate(Fig.3c) is shown regular hexagonal diffraction spot array, indicating that the two triangular faces of each nanoplate are bounded by the {111} planes. Three sets of spots could be identified based on their d-spacing: the set with the strongest intensity could be indexed to the {220} reflection of face-centered cubic (fcc) silver with a corresponding lattice spacing of 0.144 nm. The outer set with the weakest intensity is caused by reflections from {422} planes with a lattice spacing of 0.083 nm. The inner spot with a weaker intensity corresponds to the normally forbidden 1/3 {422} reflections with a lattice spacing of 0.250 nm, which implies the automically flat surface. Fig. 3d shows a typical high-resolution TEM (HTEM) image of the corner of an individual nanoplate recorded from the [$\bar{1}$11] direction. The well-resolved interference fringe pattern confirms the single crystallinity of this silver nanoplate.

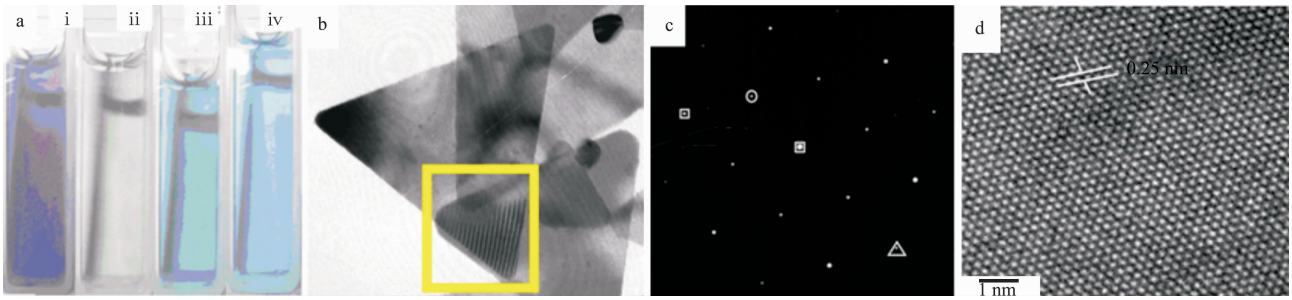

Fig.3 (a) Photos of as-prepared silver nanoplates in different sizes: (i) 100 nm, (ii) 150 nm, (iii) 200 nm and (iv) 250 nm; (b) A typical Morié pattern formed by stacking two or more nanoplates against their triangular faces (parts of the squares); (c) The electron microdiffraction pattern taken form an individual nanoplate supported on the TEM grid against one of its triangle. (the triangular silver nanoplates obtained after 48 h): the {220} reflection (squares), the {422} reflection (triangle), the 1/3{422} reflection (circle); (d) High-resolution TEM image of the corner of the an individual triangular nanoplate.

2.2 Effect of AOT concentration

To clarify the role of AOT in the growth process, we have conducted the experiments using a procedure similar to the standard conditions, except AOT concentrations. As shown in Fig.4a, Ag nanospheres with about 30 nm diameter are generated at a relatively high AOT concentration (8 mg·L^{-1}). As the concentration of AOT decreases from 4 mg·L^{-1} to 1 mg·L^{-1}, in addition to the increase of the sizes and population of triangular nanoplates, the shape becomes

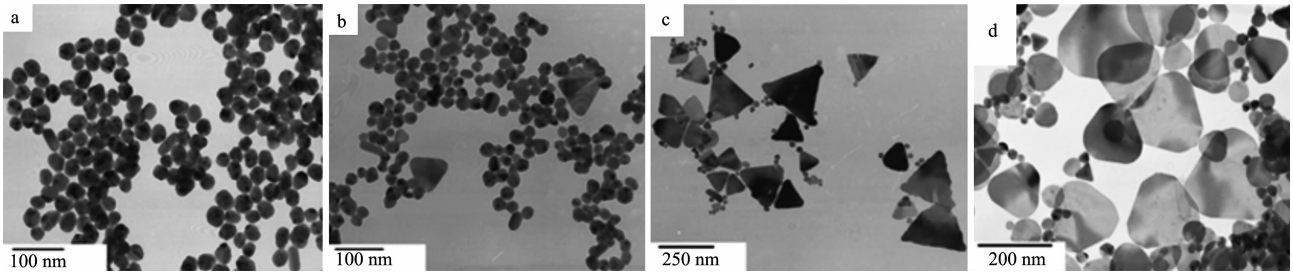

(a) 8 mg·L^{-1}; (b) 4 mg·L^{-1}; (c) 2 mg·L^{-1}; (d) 0.5 mg·L^{-1}

Fig.4 TEM images of the solutions prepared under standard conditions with different concentrations of AOT

more regular, as shown in Fig.4b, 4c and Fig.1g. The irregular silver triangular nanoplates are observed when the concentration of AOT is 0.5 mg·L^{-1}, as shown in Fig.4d. The results indicate that the concentration of AOT plays a critical role in the formation of regular triangular nanoplate. In this case, the regular triangular nanoplates are actually obtained at a relatively low AOT concentration, while the higher concentration of AOT gives a detrimental effect on the triangular nanoplate. In the surfactant system, small molecules or polymers tend to selectively adsorb on certain crystal planes to induce anisotropic growth of different planes. In our surfactant system, the much higher AOT concentration causes higher coverage of AOT on all faces of the nanoparticles, leading to an isotropic growth mode[5,7,27]. The favorite low AOT concentration causes a decrease in coverage for the highly anisotropic growth. Fig.3d displays the absorption spectra of the solutions obtained with different AOT concentrations. It is clear that the properties of UV-Vis absorption spectra are consistent with the TEM images observation (All these solutions used are not centrifugated)

2.3 Effect of pH value

Fig.5 shows TEM images of Ag anostructures prepared using a procedure similar to the standard conditions, except pH values. As shown in Fig.5a, nanoparticles with various morphologies are obtained at a higher pH value of 10. AOT was reported to be decomposed in alkaline solution [33], so it can not be capped on the surface of silver nanoparticles to control the morphology of nanoparticles, thus resulting in random growth of particles. It indicates that AOT is necessary for the formation of the triangular nanoplates. With the decrease of pH value from 8 to 5(Fig.5b-5d), the final products are irregular triangular nanoplates, triangular nanoframes, and well-shaped triangular nanoplates. The set of experiments demonstrates that the proper pH value is necessary for the formation of the perfect triangular nanoplate due to its ability to influence the environment required for the formation of triangular nanoframes by changing properties of AOT and the interaction between AOT and nanoparticles. With the proper pH value, the interaction between AOT and nanoparticles is enhanced, and thus the chemical binding sites can improve self-assembly effect of silver nanoparticles to control the growth of triangular nanoplates.

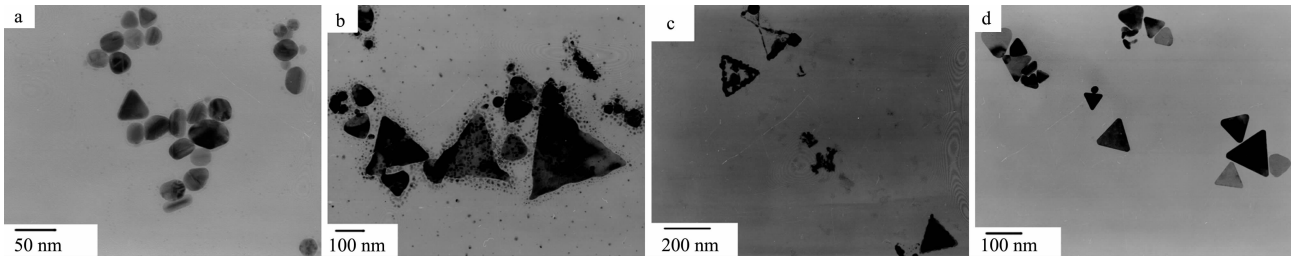

(a) pH=10; (b) pH=8; (c) pH=6; (d) pH=5

Fig.5　TEM images of the solutions prepared under stander conditions with different pH values

3 Mechanism for formation of silver triangular nanoplates

The formation of triangular silver nanoplates in the system can be explained by the mechanism of the triangular nanoframes directed growth of triangular silver nanoplates. It is evident that the concentration of AOT and other experimental conditions play decisive role in initiating the formation of triangular nanoframe. Fig.6 shows a schematic diagram outlining the plausible mechanism. In the first period, extremely small silver clusters are formed from the reduction of Ag^+. In the second period, the growth modes depend on the concentration of AOT. At the higher concentration of AOT, such as 8 mg·L^{-1}, twinned nanospheres with a large size are obtained. At a proper AOT concentration, such as 1 mg·L^{-1}, some small silver clusters capped with AOT are self-assembled into triangular nanoframes. The formation of triangular nanoframes is not clear at the moment. Two possible reasons are

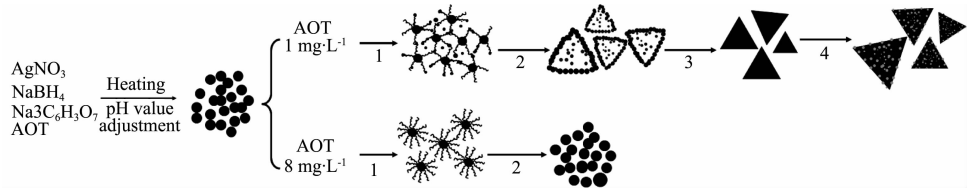

Fig.6 Schematic illustration of the formation of triangular nanoplates

suggested: one is the heating might selectively disrupt the organic layers on the surfaces of the small silver nanoparticles and make them possible to contact and assemble into the triangular nanoframes due to the interaction between the hydrophobic groups of the AOT (Molecular structure of AOT is shown in Fig.7) Another is that the application of thermal energy helps to induce activation and digest of some small nanoparticles and thus making these nanoparticles further gather into nanoframes, which is similar to Ostwald ripening. However, the exact role of AOT is still not clear. It has been speculated that the kinetics of adsorption and desorption of AOT on the crystallographic planes of the nanoparticles are different, thus leading to the eventual development of nonspherical geogemetry. Meanwhile, the proper adsorbing state of AOT on the surface of nanoparticles might also help to form self-assembled nanoparticles [26-29]. In the fourth period, triangular nanoplates are generated by the melting of the small clusters gathered in the preformed nanoframes, which serve as the template, and grow continuously to perfect triangular nanoplates, and then become larger with time. These triangular nanoplates are stable in room-temperature. In the last period, in the case of the heating and the increase in nanoplates size, some of the silver atoms, especially those located at the edges easily transport to new positions where these atoms are more favorable in energy, and will nucleate and grow to new nanoparticles adsorbed on the surface of nanoplates. At the same time, the triangular nanoplates also grow larger continuously. The above growth process corresponds well with the TEM observation and UV-Vis absorption spectra.

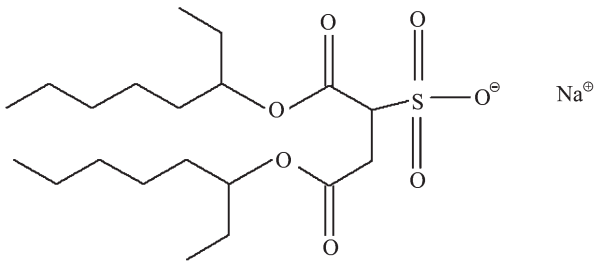

Fig.7 Molecular structure of AOT

Among five periods, the formation of the triangular nanoframes is the most significant stage to obtain regular triangular nanoplates. To further confirm the role of the nanoframes, the solution of the nanoframes (the silver colloid is centrifuged for 15 min for four times to remove the surfactants when the reaction has proceeded for 30 hr, seen in Fig.1d) is kept at ambient for 40 d. Seen from the TEM image(Fig.8), almost all of the nanoframes transform to the triangular nanoplates, indicating that the nanoframes constrain the small nanoparticles to melt, finally forming the triangular nanoplates.

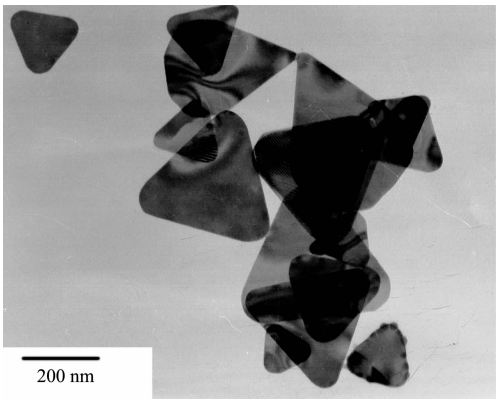

Fig.8 TEM image of triangular nanofram kept at ambient after 40 d

The silver nanoplate was first synthesized in the presence of PVP using a refluxing heating method. Xia and coworkers [7] suggested that the crystallinity of a seed and the extent of the surfactants coverage on different crystallographic planes of silver were both instrumental in controlling the morphology of the final product. They reported that triangular nanoplates with small sizes(5~15 nm) formed in the early stage served as the seeds in directing the transformation of spherical

colloids into triangular naoplates at elevated temperatures via a process similar to Ostwald ripening. However, in our experiments, we observed that the formation of triangular nanoframes as medium stage of the formation of triangular nanoplates. Self-assembly effect seems to provide a much milder driving force to facilitate the morphological evolution.

4 Conclusions

A simple and effective aqueous-phase approach is demonstrated for the large-scale synthesis of regular silver triangular nanoplates, with a thickness of 5 ~ 20 nm and the size tunable from 60 to 400 nm. The standard synthesis process involves the reduction of silver nitrate with sodium borohydride in the presence of sodium citrate and dioctyl sulfosuccinate sodium salt(AOT) as well as the heat-treatment at 60 ℃ for 36~48 h. The optical in-plane dipole plasmon band of the large silver nanoplate is extended to ~1 230 nm, which is in the near-infrared (NIR) regime. This extension has made the large nanoplates ideal for photothermally triggered drug releasing in tissues and in IR absorption or optical fiber communication. The studies of the growth process indicate that the silver triangular nanoframes are formed in the formation process, serving as templates of triangular nanoplates. The formation process of triangular nanoframes is involved with the nanoparticles assemble due to the interaction with AOT. In addition, the hearting provided the driving force to facilitate the Ostwald ripening process-growth of these triangular nanoframes at the expense of some nanoparticles and incorporation of nanoparticles. Studies from different AOT concentrations and the pH value and the reaction time demonstrate that triangular nanoframe-mediated growth mechanism works only in the proper exper imental conditions.

References:

[1] Eychmuller A. *J. Phys. Chem. B* **2001**,**104**:-6528

[2] WU Hui-Fang(武慧芳), MA Yan-Yun(马艳芸), XIE Zhao-Xiong(谢兆雄). *Chinese Sci. Bull.*(*Kexue Tongbao*), **2007**,**52**: 2217-2219

[3] LIU Xia(刘　霞), HE Tian-Jing(何天敬), CHEN Dong-Ming (陈东明), et al. *Acta Phys.-Chim. Sin.*(*Wuli Huaxue Xuebao*), **2005**,**18**:81-86

[4] SHAO Li(邵　丽), WANG Xi-Kui(王西奎), WANG Jin-Gang (王金刚). *Chinese J. Inorg. Chem.* (*Wuji Huaxue Xuebao*), **2007**,**23**:1823-1828

[5] Sun Y, Yin Y Y, Xia Y, et al. *Chem. Mater.*, **2002**,**14**:4736-4745

[6] Xiong Y, McLellan J M, Xia Y, et al. *J. Am. Chem. Soc*., **2005**, **127**:17118-17121

[7] Sun Y, Xia Y. *Nano Lett*., **2003**,*3*:675-679

[8] Wiley B, Sun Y, Xia Y J, et al. *Chem. Eur*., **2005**,**11**:454-463

[9] Murphy C J, Jana N R. *Adv. Mater*., **2002**,**14**:80-82

[10]Wiley B, Herricks T, Su Y, et al. *Nano Lett*., **2004**,**4**:1733-1739

[11]Jiang L P, Zhu J M, Chen H Y, et al. *Inorg. Chem.*, **2004**,**43**: 5877-5883

[12]Chen S, Carroll D L. *Nano Lett.*, **2002**,**2**:1004-1007

[13]Pastorize-Santos I, Liz-Marzan L M. *Nano Lett*., **2002**,**2**:903-905

[14]Lofton C, Sigmund W. *Adv. Funct. Mater*., **2005**,**15**:1197-1208

[15]Sun Y, Xia Y. *Adv. Mater.*, **2003**,**15**:695-699

[16]Jin R, CaoY, Zheng J G, et al. *Science*, **2001**,**294**:1901-1903

[17]Maillard M, Huang P, Brus L. *Nano Lett*., **2003**,**3**:1611-1615

[18]He R, Qian X, Zhu Z, et al. *J. Mater. Chem.*, **2002**,**12**:3783-3786

[19]He R, Qian X, Zhu Z, et al. *Chem. Phys. Lett.*, **2003**,**369**:454-458

[20]Callegari A, Tonti D, Chergui M. *Nano Lett.*, **2003**,**3**:1565-1568

[21]Chen S, Fan Z, Carroll D L. *J. Phys. Chem. B*, **2002**,**106**: 10777-10781

[22]Yener D O, Sindel J, Adair J H, et al. *Langmuir*, **2002**,**18**: 8692-8699

[23]Pieni M, Gulik-Krzywicki T, Dedieu J, et al. *Langmuir*, **1998**,**14**:7359-7363

[24]Filankembo A, Pileni M. *Appl. Surf. Sci*., **2000**:164260

[25]Jana N, Gearheart L, Murphy C. *Adv. Mater*., **2001**,**13**:1389-1993

[26]Wiley B J, Xiong Y J, Xia Y, et al. *Nano Lett*., **2006**,**6**:765-768

[27]Chen S, Carroll D L. *Nano Lett*., **2002**,**2**:1003-1007

[28]Chen S, Carroll D L. *J. Phys. Chem. B*, **2004**,**108**:5500-5506

[29]Lofton C, Sigmund W. *Adv. Funct. Mater*., **2005**,**15**:1197-1208

[30]Thomas K G, Barazzouk S, Kamat P V, et al. *J. Phys. Chem. B*, **2004**,**108**:13066-13068

[31]Chalmers J M, Griffiths P R, Eds. *Handbook of Vibrational Spectroscopy*. New York: Wiley, **2002**.759-774